SUPPLEMENTAL MATERIALS

Optimization of a Cardiomyocyte Model Illuminates Role of Increased I_{NaL} in Repolarization Reserve

Kristin E Fullerton[1,3], Alexander P. Clark[2], Trine Krogh-Madsen[3,4], and David J Christini[5]

[1]Physiology, Biophysics and Systems Biology Program, Weill Cornell Graduate School of Medical Sciences, New York, NY, USA
[2]Department of Biomedical Engineering, Cornell University, Ithaca, New York, USA.
[3]Department of Physiology & Biophysics, Weill Cornell Medicine, New York, NY, USA.
[4]Institute for Computational Biomedicine, Weill Cornell Medicine, New York, NY, USA.
[5]SUNY Downstate Health Sciences University, Brooklyn, NY, USA

1 Model Updates

Since the GB model does not include late sodium, the I_{NaL} equations were extracted from the ToR-ORd model source code and added to the GB model. The late sodium conductance parameter was scaled by the ratio of peak sodium between both models (356 A/F (GB) / 294 A/F (ToR-ORd)). Lastly, CaMKII phosphorylation was added to the GB model as well since the ToR-ORd I_{NaL} formulation is dependent on it.

1.1 Definitions and Abbreviations

parameter	model code variable	definition
$m_{L,\infty}$	mLss	steady state activation for I_{NaL}
$\tau_{m,L}$	tmL	time constant of gate m
m_L	mL	activation for I_{NaL}
$h_{L,\infty}$	hLss	steady state inactivation for I_{NaL}
$\tau_{h,L}$	thL	time constant of gate h
h_L	hL	inactivation for I_{NaL}
$h_{L,CaMK,\infty}$	hLssp	steady state inactivation for CaMK phosphorylated I_{NaL}
$\tau_{h,LCaMK}$	thLp	time constant of h gate phosphorylated
$h_{L,CaMK}$	hLp	inactivation for CaMK phosphorylated I_{NaL}
$\phi_{INaL,CaMK}$	fINaLp	fraction of I_{NaL} channels phosphorylated by CaMK
G_{NaL}	GNaL	maximum conductance of INaL
$I_{NaL,junc}$	INaL_junc	current through I_{NaL} channels in the junctional space
$I_{NaL,sl}$	INaL_sl	current through I_{NaL} channels in the subsarcolema space
I_{NaL}	INaL	current through I_{NaL} channels
α_{CaMK}	aCaMK	phosphorylation rates of CaMK
β_{CaMK}	bCaMK	dephosphorylation rates of CaMK
$CaMK_0$	CaMKo	fraction of active CaMK binding sites at equilibrium
$CaMK_{active}$	CaMKa	fraction of active CaMK binding sites
$CaMK_{bound}$	CaMKb	fraction of CaMK binding sites bound to Ca^{2+}/calmodulin
$CaMK_{trap}$	CaMKt	fraction of autonomous CaMK binding sites with trapped calmodulin

1.2 Initial condition additions

$$m_L = 0.0001629$$

$$h_L = 0.5255$$

$$h_{L,CaMK} = 0.2872$$

$$CaMK_{trap} = 0.0111$$

1.3 I_{NaL}

$$m_{L,\infty} = \frac{1}{1 + e^{\frac{-V-42.85}{5.264}}}$$

$$\tau_{m,L} = 0.1292 * e^{-(\frac{V+45.79}{15.54})^2} + 0.06487 * e^{-(\frac{V-4.823}{51.12})^2}$$

$$\frac{d(m_L)}{dt} = \frac{m_{L,\infty} - m_L}{\tau_{m,L}}$$

$$h_{L,\infty} = \frac{1}{1 + e^{\frac{V+87.61}{7.488}}}$$

$$\tau_{h,L} = 200ms$$

$$\frac{d(h_L)}{dt} = \frac{h_{L,\infty} - h_L}{t_{h,L}}$$

$$h_{L,CaMK,\infty} = \frac{1}{1 + e^{\frac{V+93.81}{7.488}}}$$

$$\tau_{h,LCaMK} = 3 * \tau_{h,L}$$

$$\frac{d(h_{L,CaMK})}{dt} = \frac{h_{L,CaMK,\infty} - h_{L,CaMK}}{\tau_{h,LCaMK}}$$

$$\phi_{INaL,CaMK} = \frac{1}{1 + \frac{0.15}{CaMK_{active}}}$$

$$G_{NaL} = 0.029 * \frac{356}{294} \frac{mS}{\mu F}$$

$$I_{NaL,junc} = G_{NaL} * (V - E_{Na_{junc}}) * m_L * ((1 - \phi_{INaL,CaMK}) * h_L + \phi_{INaL,CaMK} * h_{L,CaMK})$$

$$I_{NaL,sl} = G_{NaL} * (V - E_{Na_{sl}}) * m_L * ((1 - \phi_{INaL,CaMK}) * h_L + \phi_{INaL,CaMK} * h_{L,CaMK})$$

$$I_{NaL} = I_{NaL,junc} + I_{NaL,sl}$$

where $E_{Na_{junc}}$ and $E_{Na_{sl}}$ are the Nerst potentials for sodium in the junctional and subsarcolemmal compartments, respectively. The equations for these two parameters were not changed in respect to the baseline BM model and can be found in the supplmetary material of Grandi et al. [**grandi˙novel˙2010**].

1.4 CaMK

$$\alpha_{CaMK} = 0.05 \text{ ms}^{-1}$$

$$\beta_{CaMK} = 0.00068 \text{ ms}^{-1}$$

$$CaMK_0 = 0.05$$

$$CaMK_{bound} = CaMK_0 * \frac{1 - CaMK_{trap}}{1 + \frac{0.0015}{Ca_i}}$$

$$CaMK_{active} = CaMK_{bound} + CaMK_{trap}$$

$$\frac{d(CaMK_{trap})}{dt} = \alpha_{CaMK} * CaMK_{bound} * (CaMK_{bound} + CaMK_{trap}) - \beta_{CaMK} * CaMK_{trap}$$

where Ca_i is intracellular calcium which was not changed in respect to the baseline GB model.

2 Supplemental Figures

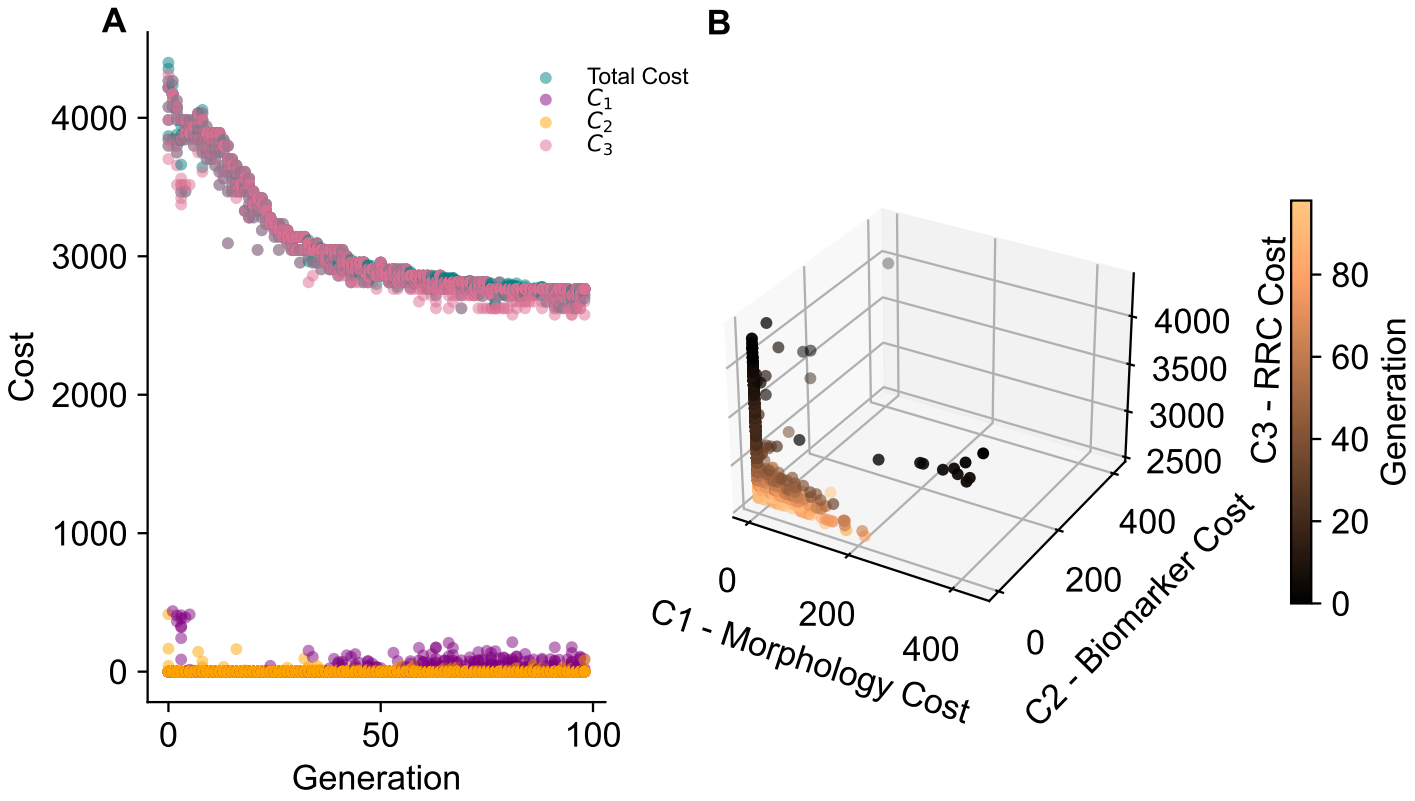

Figure S 1: Evolution of the best individuals in GA optimization and their respective cost components. A. The total cost of the best individual at each generation and its respective components (C_1, C_2, and C_3) are plotted for all 8 GA runs. Therefore, 32 (4 cost terms x the best individual from all 8 GA trials) points are plotted for each generation. B. The best individual in each generation from all 8 GA trials plotted by its C_1, C_2, and C_3 values which sum to calculate the total cost. Each point is colored by generation.

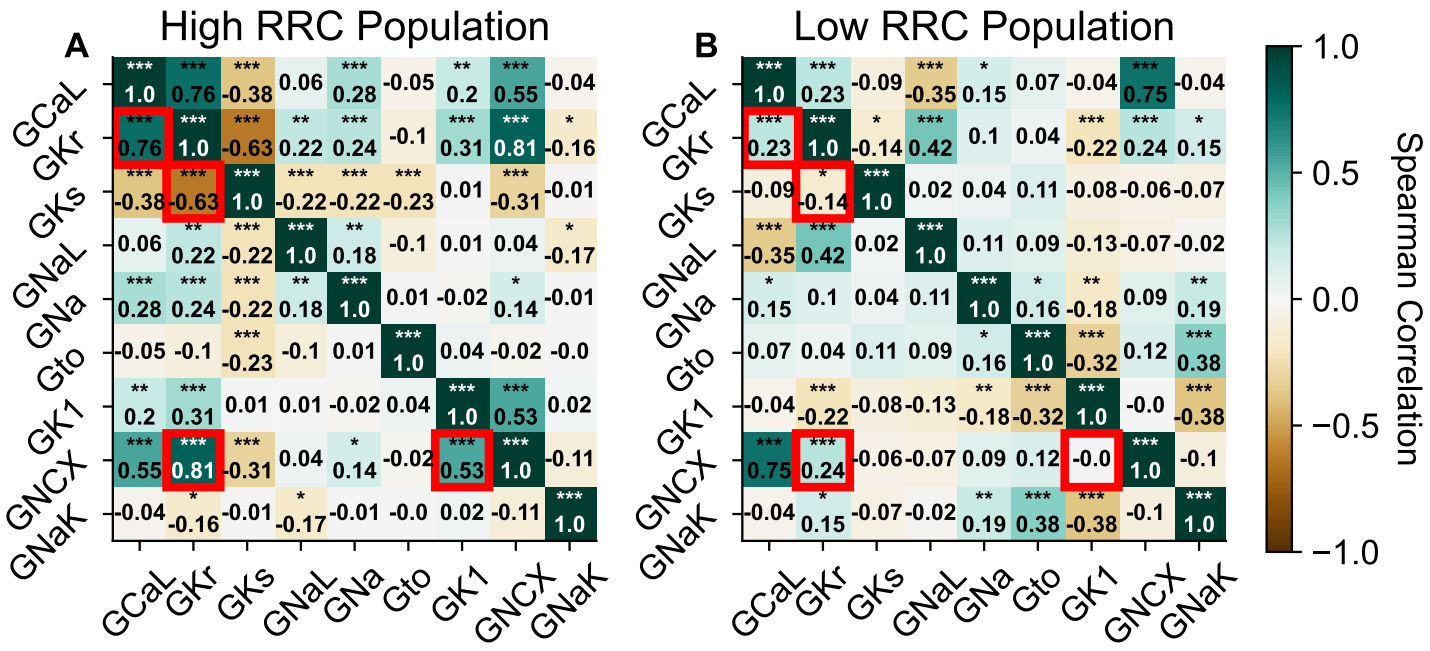

Figure S 2: Correlations between specific ion-channels are present in a group of cells with high RRC size but not in a group with low RRC. Spearman correlations between all nine ion-channel profile conductances for a population of models with A. high and B. low RRC magnitude. The high RRC population is the 220 best individuals present in all generations of all 8 GA trials. These individuals all have a C_3 error below 2800. The population of models with low RRC represent the 233 worst individuals present in all generations of all 8 GA trials. These individuals all have a C_3 error greater than 5200. The red box highlights strong correlations in A that are not present in B.

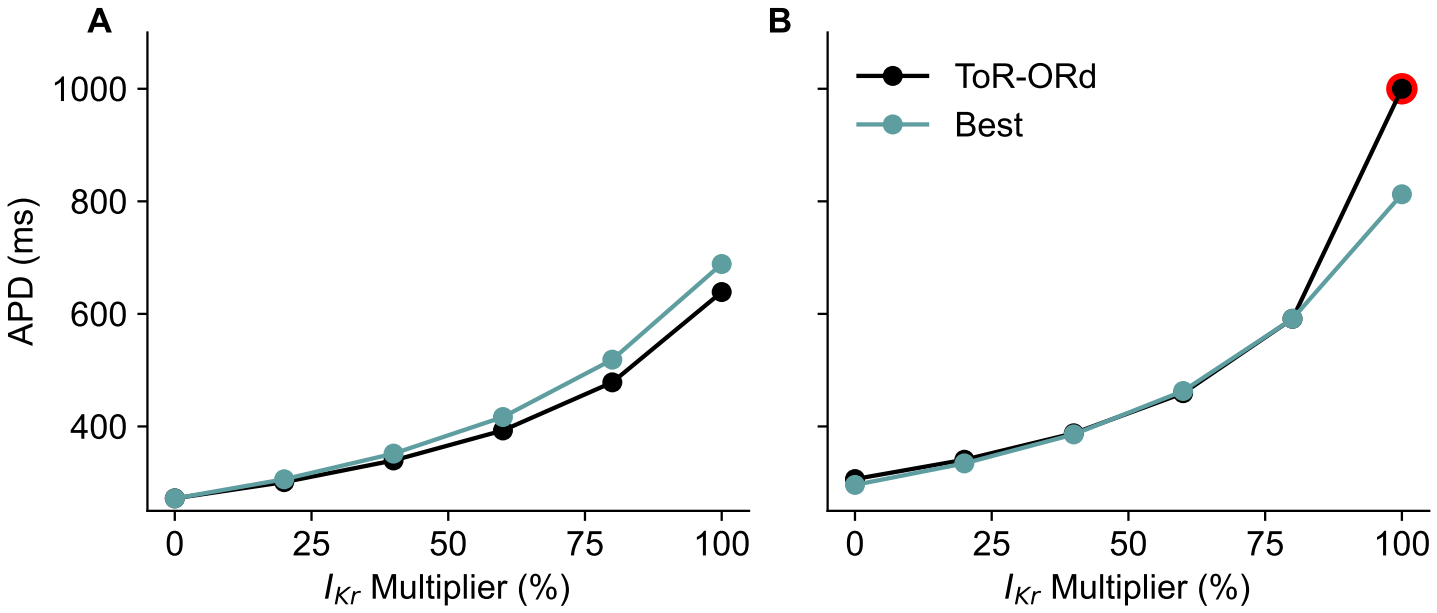

Figure S 3: Evaluation of APD after I_K perturbations. A. APD value after 0, 20%, 40%, 60%, 80%, and 99% IKr block. B. The same analysis as A was repeated but with an additional block of the background potassium channel (I_{Kb}). The perturbations were applied to both the baseline ToR-ORd model (black) and a representative optimized model. The red circle represents a simulation with a repolarization abnormality.